Senescent Human Fibroblasts Increase the Early Growth of Xenograft Tumors via Matrix Metalloproteinase Secretion

Dan Liu and Peter J. Hornsby

Department of Physiology and Sam and Ann Barshop Institute for Longevity and Aging Studies, University of Texas Health Science Center, San Antonio, Texas

Abstract

Although cellular senescence is believed to have a tumor suppressor function, senescent cells have been shown to increase the potential for growth of adjacent cancer cells in animal models. Replicatively senescent human fibroblasts increase the growth of cotransplanted cancer cells *in vivo*, but the role of cells that have undergone damage-mediated stress-induced premature senescence (SIPS) has not been studied in mouse transplant models. Here, we show that human fibroblasts that have undergone SIPS by exposure to the DNA-damaging agent bleomycin increase the growth of cotransplanted cancer cells (MDA-MB-231) in immunodeficient mice. Xenografts containing SIPS fibroblasts (SIPSF) exhibited early tissue damage as evidenced by fluid accumulation (edema). Cancer cells adjacent to the fluid showed increased DNA synthesis. Fluid accumulation, increased xenograft size, and increased cell proliferation were all reduced by the matrix metalloproteinase (MMP) inhibitor GM6001. MMPs and other genes characteristic of inflammation/tissue injury were overexpressed in SIPSF. Inhibition of MMP activity did not affect SIPSF stimulation of cancer cell proliferation in culture. However, another overexpressed product (hepatocyte growth factor) did have a direct mitogenic action on cancer cells. Based on the present results, we propose that senescent cells may promote cancer growth both by a direct mitogenic effect and by an indirect effect via tissue damage. Senescent stromal cells may cause an MMP-mediated increase in permeability of adjacent capillaries, thereby exposing incipient cancer cells to increased levels of mitogens, cytokines, and other plasma products. This exposure may increase cancer cell proliferation and result in promotion of preneoplastic cells. [Cancer Res 2007;67(7):3117–26]

Introduction

The senescent state is an alternative fate to cell death in cells that have suffered damage to their DNA that they cannot repair (1, 2). Although first described as the terminal state of cells with telomere dysfunction, recognized by the cell as a form of DNA damage, cellular senescence is now understood to be a general reaction of cells to a wide range of unrepairable DNA damage and may serve as a tumor suppressor mechanism (3–5). Senescent cells occur in tissues *in vivo* under various conditions (2). Although senescent cells accumulate in aging, they are also present in a variety of pathologic conditions such as chronic ulcers, benign prostatic hypertrophy, and tissues damaged by radiation or chemotherapy (3, 4, 6).

Senescent cells exhibit a large range of changes in gene expression that resembles the acute inflammatory response of fibroblasts in tissues reacting to tissue injury (2). Probably as a consequence of these changes, senescent human fibroblasts are unable to reconstitute artificial skin of normal structure; skin transplants reconstituted with senescent fibroblasts exhibited increased splitting or blistering at the dermal/epidermal junction in comparison with skin reconstituted with control fibroblasts (7). Among the changes in gene expression in senescent cells, the overexpression of matrix metalloproteinases (MMP) is striking (8–10). MMPs are involved in a wide variety of reactions to tissue injury. Tissue damage is accompanied by increased permeability of capillaries, the recruitment of inflammatory cells, and the release of inflammatory mediators and cytokines (11). Increased microvascular permeability may cause localized or more widespread accumulation of extracellular fluid (edema). Many of these changes are greatly reduced when the activity of MMPs is inhibited (11). Direct injection of MMPs into tissues causes damage that includes increased capillary permeability and edema (12).

Disruption of the extracellular matrix by MMPs is increasingly recognized as a critical factor in the initiation of cancer (13–18). Most of the MMPs in developing cancers are produced by stromal fibroblasts within tumors rather than by tumor cells (13, 19). These secreted enzymes degrade the extracellular matrix and thereby change the tumor cell microenvironment (20, 21).

The role of stromal fibroblasts has been studied in xenograft models in which tumorigenic or nontumorigenic cells are cotransplanted together with fibroblasts in immunodeficient mice (22–25). Cotransplanted stromal cells not only increase the survival and growth of tumor cells but also enhance the survival and function of nontumorigenic cells in cell transplants and tissue recombination models (26–29). With respect to cancer cell xenografts, early experiments showed that cotransplanted fibroblasts stimulated the initial "take" of tumors but did not affect the rate of growth of the tumors once established (24, 25).

Subsequently, cotransplantation xenograft models in immunodeficient mice were used to show that senescent fibroblasts exert a much greater effect on xenograft tumor growth than nonsenescent fibroblasts (30). This important result has two major implications. First, major mediators of the effects of cotransplanted fibroblasts on xenograft tumor growth are likely to comprise enzymes or other molecules that are produced in excess by senescent cells, such as MMPs. This is consistent with prior work showing that the growth-enhancing effects of nonsenescent fibroblasts in xenografts is reduced when their ability to produce MMPs is inhibited (31). Second, because senescent cells cannot divide, the effect on growth must be exerted by only the initial population of transplanted fibroblasts. Probably, transplanted fibroblasts, even if not senescent, rapidly become diluted by the growth of the cancer cells. As

Requests for reprints: Peter J. Hornsby, University of Texas Health Science Center, STCBM Building, 15355 Lambda Drive, San Antonio, TX 78245. Phone: 210-562-5080; Fax: 281-582-3538; E-mail: hornsby@uthscsa.edu.

doi:10.1158/0008-5472.CAN-06-3452

the tumor grows, fibroblasts derived from the host immunodeficient mouse become integrated into the tumor; the critical role of the stromal compartment of cancers for determining the growth and invasiveness of the tumor is well established (13, 17). Host stromal cells therefore exert effects at later times of xenograft growth. The enhancement of tumor growth by senescent fibroblasts may be one component of the important role of inflammatory processes and chronic tissue damage in the initiation and growth of cancers (32).

These prior results are consistent with the following model: (*a*) senescent fibroblasts increase survival and/or proliferation of transplanted tumor cells by some action that occurs in the very early phase of xenograft growth; (*b*) they exert this action via the secretion of products that are overexpressed by senescent cells, such as MMPs. In the present experiments, we employed a xenograft model in immunodeficient mice to investigate the mechanism of action of senescent fibroblasts on experimental tumor growth. We looked for morphologic changes in xenografts with cotransplanted senescent cells consistent with an inflammatory/tissue injury reaction within the xenograft, and we investigated whether senescent fibroblasts exert their growth stimulatory effect in xenografts via the secretion of MMPs. The experimental system employed here is a s.c. transplant of MDA-MB-231 cells and fibroblasts that have undergone stress-induced premature senescence (SIPS), defined as senescence resulting from forms of damage other than telomere shortening. We chose MDA-MB-231 cells because it has been well established that growth of this cell type responds to fibroblast cotransplantation (24, 25). The SIPS model used comprised fibroblasts with unrepairable DNA damage resulting from exposure to bleomycin. Cells with bleomycin-induced DNA damage enter a state of irreversible growth arrest that is similar to that found in other senescence models and overexpress the inflammatory/tissue injury genes that are characteristic of senescent cells, including MMPs (33–36). We chose to use HCA2 human neonatal fibroblasts (37) because in preliminary studies, we showed that replicatively senescent HCA2 cells (i.e., cells made senescent by telomere shortening) stimulated MDA-MB-231 xenograft growth, confirming earlier experiments using WI-38 fetal lung fibroblasts (30).

Materials and Methods

Cell culture. Normal human newborn foreskin fibroblasts (HCA2 and HCA3) were obtained from Dr. Olivia Pereira-Smith (University of Texas Health Science Center at San Antonio). Green fluorescent protein (GFP)–expressing HCA3 cells were obtained by infection with retrovirus pLEGFP-N1 (BD Biosciences Clontech, Palo Alto, CA). Human breast cancer cells MDA-MB-231 were obtained from Dr. Judith Campisi (Lawrence Berkeley National Laboratory). GFP-expressing MDA231 cells were obtained by transfection with plasmid pEGFP-N1 (Clontech). GFP-expressing human hepatoma Hep3B cells were obtained by infection with retrovirus pLEGFP-N1. YFP-expressing human prostate cancer PC-3 cells were obtained from Dr. Bandana Chatterjee (University of Texas Health Science Center at San Antonio). All cells were cultured in DMEM supplemented with 10% cosmic calf serum (Hyclone Laboratories, Logan, UT). GFP-expressing immortalized bovine adrenocortical cells (BAC-hTert) were cultured in a specialized medium as previously described (38).

Preparation of SIPS fibroblasts. Senescence was induced in HCA2 fibroblasts by incubation in 10 μg/mL bleomycin sulfate (Fluka, Buchs, Switzerland) for 24 h (33, 35, 36). Following this treatment, cells had an enlarged, flattened, senescence-like morphology. Senescence was evidenced by plating cells at low density and showing the absence of colony growth and was also assessed by senescence-associated β-galactosidase (SA-βgal) staining (39). SIPS fibroblasts (SIPSF) were used for experiments after 7 days of incubation in regular medium following 24 h of incubation in bleomycin. Additionally, SIPSF were compared with irradiated fibroblasts in some experiments. Irradiation was done by exposure of cells to a ^{137}Cs source (44 Gy).

Preparation of xenografts in immunodeficient mice. ICR *scid* mice originally purchased from Taconic (Germantown, NY) were maintained in an animal barrier facility as a breeding colony. Animals (both males and females) at an age greater than 6 weeks (~25 g body weight) were used in these experiments. Procedures were approved by the institutional animal care committee and were carried out in accordance with the NIH Guide for the Care and Use of Laboratory Animals. The cell transplantation procedure was done under tribromoethanol anesthesia (28).

Collagen was prepared as described previously from rat tail collagen fibers (40). Before use, the ice-cold collagen solution was neutralized and adjusted to the proper osmolarity by adding a mixture of NaOH and ×10 DME. The cells to be transplanted were centrifuged. The cell pellet (~40 μL) was mixed with 40 μL collagen solution. The cell/collagen mixture was maintained at 4°C. Before the cells were transplanted, the cell/collagen mixture was taken up into a 200-μL pipette tip, and the mixture was allowed to partially gel for 3 min at room temperature. An incision of about 1 to 2 mm was made in the skin at the base of the ear. A pocket beneath the skin was formed using forceps. A silk 6-O suture was introduced around the skin opening. The mixture was then injected into the s.c. pocket, and the suture was tightened to prevent leakage of cells from the transplantation site.

In some experiments, the broad spectrum MMP inhibitor GM6001 (Calbiochem, La Jolla, CA) was incorporated into xenografts as follows: 100 μmol/L GM6001 or 0.8% DMSO (vehicle) was mixed into the cell/collagen mixture at 4°C. The mixture was then taken up into a pipette tip and transplanted as described above.

Monitoring growth of xenografts. Postoperative care for the animals, including the administration of analgesics and antibiotics, was as previously described (28). The growth of xenografts was assessed at intervals using calipers. Tumor volumes were calculated by the following formula: volume = $0.5 \times \text{width}^2 \times \text{length}$. In some experiments, we monitored the survival of cotransplanted GFP-expressing fibroblasts by photography of xenografts under illumination by 470-nm light (Lightools Research, Encinitas, CA). Animals were sacrificed at various times following transplantation, as described in Results.

Measurement of MMP activity. MMP activity in conditioned medium was measured by zymography. Conditioned medium samples were collected and concentrated by centrifugal filter devices (Millipore, Bedford, MA). Concentrated protein (50–60 μg) was loaded into NOVEX 12% zymogram casein gels (Invitrogen, Carlsbad, CA). Proteins were electrophoresed in Tris/glycine SDS running buffer under nondenaturing conditions. Gels were washed thrice in 2.5% (v/v) Triton X-100 for 30 min at room temperature to remove SDS. Zymograms were subsequently developed by incubation for 48 h at 37°C in zymogram reaction buffer [0.2 mol/L NaCl, 5 mmol/L $CaCl_2$, 40 mmol/L HCl, 50 mmol/L Tris, 0.02% Brij 35 (pH 7.1)]. Gels were stained with Coomassie blue. Enzymatic activity was visualized as a clear band against a dark background of stained casein.

Histology and immunohistochemistry. Xenografts were fixed in 4% paraformaldehyde and processed conventionally. For bromodeoxyuridine (BrdUrd) labeling, 100 mg/kg BrdUrd was administered to mice i.p. 22 h before sacrifice. Staining of nuclei with incorporated BrdUrd was done as previously described (40). Sections were lightly counterstained with hematoxylin. Immunostaining of GFP and Ki-67 and detection of apoptotic cells by *in situ* oligo ligation were done as previously described (38, 41).

Real-time PCR. RNA was isolated from cultured cells using RNA-Bee (Tel-Test, Friendswood, TX) according to the manufacturer's directions. For reverse transcription, 4 μg RNA was used in a reaction with random hexamer primers and Superscript II reverse transcriptase (Invitrogen; 200 units) for 50 min at 42°C. Primers used were those predicted as optimal by the program Primer Express (Applied Biosystems, Foster City, CA). The PCR protocol was that recommended for the ABI 7900HT Fast Real-time PCR System (Applied Biosystems). Accumulation of PCR products was measured by SYBR green fluorescence (SYBR green master mix; Applied Biosystems).

For each RNA sample, four cDNA concentrations were assayed, each cDNA concentration being used in triplicate reactions. The analysis of the raw data was done using SDS software from the manufacturer. The number of cycles required to reach the threshold level of PCR product (C_t) was determined. For each sample, $C_{t(gene)} - C_{t(\beta\text{-actin})}$ was calculated, and this value was used to calculate the ratio of gene mRNA/β-actin mRNA.

Antibody arrays. Conditioned medium samples (1 mL) were used in incubations with antibody array membranes (human MMP antibody array and human atherosclerosis cytokine array; Raybiotech, Norcross, GA). The membranes were washed and incubated with a secondary biotin-conjugated antibody followed by incubation with horseradish peroxidase–conjugated streptavidin. The membranes were developed by using enhanced chemiluminescence and were exposed to X-ray film.

ELISA for hepatocyte growth factor. Conditioned medium samples were assayed by the human hepatocyte growth factor (HGF) Quantikine ELISA kit (R&D Systems, Minneapolis, MN) according to the manufacturer's instructions.

Coculture experiments. SIPS HCA2 fibroblasts (5×10^5) or control fibroblasts (2.5×10^5) were seeded into 6-cm dishes to generate 90% to 100% confluent fibroblast monolayers. After 2 days of incubation in serum-containing medium, the control fibroblasts had increased in number to $\sim 5 \times 10^5$. Fibroblast monolayers were incubated for 36 h in serum-free medium before coculture experiments began. MDA231-GFP, Hep3B-GFP, or PC-3-YFP ($1–2 \times 10^4$) cells were seeded in 6-cm culture dishes or onto the fibroblast monolayers. These cells had also been maintained in serum-free medium before the coculture experiment. MDA231-GFP/fibroblast cocultures were maintained in serum-free DMEM supplemented with 5 μg/mL insulin. Hep3B-GFP/fibroblast and PC-3-YFP/fibroblast cocultures were maintained in DMEM supplemented with 0.2% cosmic calf serum. Each group comprised three replicates, and the experiment was repeated at least thrice. For coculture of immortalized bovine adrenocortical cells (BAC-hTert) and fibroblasts, the procedures followed the above protocol except that BAC-hTert cells were incubated in specialized medium (26, 28) overnight following seeding on fibroblast lawns and then changed to DMEM supplemented with 0.1% cosmic calf serum and 5 μg/mL insulin. The proliferation of fluorescent cells was quantified by an on-chip flow cytometry method (Agilent Bioanalyzer, Agilent Technologies, Santa Clara, CA). In some experiments, 25 μmol/L MMP inhibitor GM6001 or 1% DMSO (vehicle) were added to the culture medium. Also in some experiments, we added 20 μg/mL mouse monoclonal anti-HGF neutralizing antibody (clone 24612; R&D Systems), 20 μg/mL mouse IgG1 isotype control (clone 11711; R&D Systems), or 20 μg/mL anti-HGF antibody combined with 200 ng/mL recombinant human HGF (R&D Systems).

Results

Stimulation of xenograft tumor growth by SIPSF is accompanied by early fluid accumulation. We transplanted MDA231 cells s.c. in *scid* mice, either alone or mixed with equal numbers of SIPSF or control fibroblasts. By 8 days following cell transplantation, it was possible to palpate solid nodules beneath the skin and measure their size externally with calipers (Fig. 1*A*). Caliper measurements showed that MDA231/SIPSF xenografts were significantly larger than MDA231/CF and MDA231 xenografts at 8 days. Before this, at 4 days, accurate estimation of size by external caliper measurements was not possible, but palpation showed that the larger MDA231/SIPSF xenografts were soft cystic structures. To investigate the structure of early xenografts, we sacrificed animals bearing xenografts of three types (MDA231/SIPSF, MDA231/CF, and MDA231 alone) at 5 days following cell transplantation. The histologic structure of MDA231/SIPSF xenografts was strikingly different from that of MDA231/CF and MDA231 xenografts. The presence of a central fluid-filled region in MDA231/SIPSF xenografts accounted for the soft cystic nature of these transplants that was noted by external palpation. A peripheral layer of cells surrounded a central accumulation of fluid. Fluid accumulation was much less prominent in MDA231/CF xenografts and was only occasionally seen in xenografts formed from MDA231 cells alone. Images of histologic sections were used to measure volumes of entire xenografts and the volumes of the fluid and solid portions (Fig. 1*A, inset*). The solid portions of the xenografts were significantly larger in both the MDA231/SIPSF and MDA231/CF groups; note that these xenografts would be anticipated to be larger at early times because the total number of cells transplanted was greater in the two groups with cotransplanted fibroblasts. However, the most notable difference was that the fraction of the entire transplant occupied by fluid was much greater in MDA231/SIPSF xenografts than in MDA231/CF or MDA231 alone; increased fluid volume accounted for most of the difference in size between MDA231/SIPSF and MDA231/CF xenografts.

At 5 days, the solid portions of the xenografts comprised loosely adhering cells that were often spindle shaped (Fig. 1*B*). Using the pan-macrophage marker F4/80, we found more macrophages in tumors at 5 days than at later time points (data not shown). By 9 days, most fluid had disappeared, and the solid portions of the xenografts were in all cases larger. The tissue still comprised loosely attached irregularly shaped cells (Fig. 1*C*). After day 9, the xenografts entered a period of rapid enlargement; MDA231/SIPSF xenografts were significantly larger as assessed by caliper measurements at days 16 and 20. At 19 days, xenografts comprised solid tumor tissue comprising densely packed round cells (Fig. 1*D*). As the tumors became very large, the rate of growth decreased and differences among the groups were not significant on day 25.

An optimal effect of senescent fibroblasts required equal numbers of cancer cells and senescent fibroblasts (2×10^6 each). A stimulatory effect of senescent fibroblasts was still observed when fewer (2×10^5) cancer cells were used; no additional stimulatory effect was observed when greater numbers of fibroblasts were used (data not shown).

These data suggest that SIPSF promote the initial growth of xenograft tumors as a result of a form of tissue damage that is characterized by fluid accumulation within the tumor. The effect of SIPSF on early-stage tumor growth and fluid accumulation was not specific to MDA231 tumors. Human prostate cancer cell PC-3 cells when transplanted with SIPSF also exhibited greater fluid accumulation and larger tumor sizes on day 5 than control groups (data not shown). Additionally, we studied MDA231 xenografts formed with SIPSF in sites other than the s.c. site at the base of the ear. Xenografts formed in other s.c. sites and within skeletal muscles also showed fluid accumulation when xenografts were formed with SIPSF but not with control fibroblasts or with cancer cells alone.

The data presented above showed that the solid portions of MDA231/SIPSF xenografts were not very different in size from MDA231/CF xenografts at day 5; yet, several days later, when the xenografts enter a period of rapid growth, MDA231/SIPSF xenografts grew significantly more rapidly. This indicates that tumor cells within MDA231/SIPSF xenografts either proliferate more rapidly or have a lower rate of cell death. We tested this by administering BrdUrd to animals bearing xenografts before sacrifice. In 5-day MDA231/SIPSF xenografts, BrdUrd-positive proliferating cells were most often found in the solid tissue adjacent to the fluid in the center of the xenograft (Fig. 2*A*). There were significantly more proliferating cells in MDA231/SIPSF xenografts than in MDA231/CF or MDA231 xenografts.

We also measured apoptotic cells in early xenografts using a specific visualization method (*in situ* oligo ligation). There were very

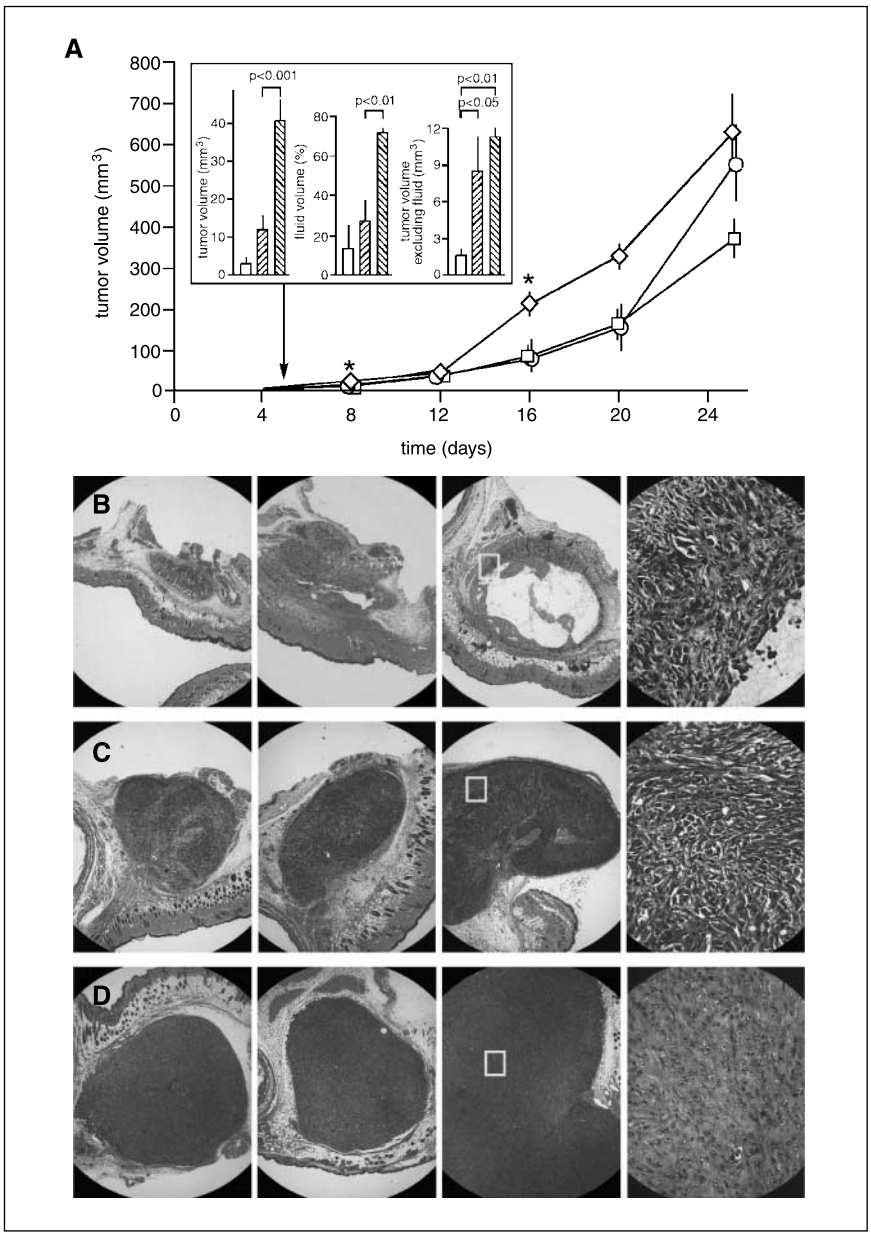

Figure 1. Stimulation of xenograft tumor growth in immunodeficient mice by SIPSF is accompanied by early fluid accumulation. *A,* size of xenografts measured externally using calipers (n = 6 per group). ○, 2 × 10^6 MDA231 cells transplanted alone; □, 2 × 10^6 MDA231 cells cotransplanted with 2 × 10^6 control HCA2 human fibroblasts (*CF*); ◇, 2 × 10^6 MDA231 cells cotransplanted with 2 × 10^6 SIPSF. *, at day 8, MDA231/SIPSF xenografts were significantly larger than MDA231/CF xenografts (P < 0.05) and MDA231 xenografts (P < 0.01); at days 16 and 20, MDA231/SIPSF xenografts were significantly larger than both MDA231/CF and MDA231 xenografts (P < 0.05). *Inset,* relationship between tumor volume and fluid volume in MDA231 xenografts at 5 d following cell transplantation; *open columns,* MDA231 xenografts; *first hatched columns,* MDA231/CF xenografts; *second hatched columns,* MDA231/SIPSF xenografts. *B,* H&E-stained sections of representative xenografts from mice sacrificed at 5 d following transplantation (*left* to *right,* MDA231 xenografts, MDA231/CF xenografts, MDA231/SIPSF xenografts; *yellow rectangle,* enlargement of area). Magnification, ×40 except for enlargement (×400). *C,* sections of representative xenografts from mice sacrificed at 9 d following transplantation. *D,* sections of representative xenografts from mice sacrificed at 19 d following transplantation.

few apoptotic cells in all types of xenografts (Fig. 2*C*). The low numbers of apoptotic cells and the increased BrdUrd labeling in MDA231/SIPSF xenografts indicate that SIPSF exert a positive effect on tumor cell proliferation, rather than by inhibiting apoptosis. The location of proliferating cells near the fluid center of the xenograft strengthens the hypothesis that the accumulation of fluid is causatively related to the growth stimulatory effects of SIPSF.

SIPSF stimulate growth of primary human cells with defined genetic alterations. We investigated whether SIPSF could increase the growth of xenografts formed from primary human cells with defined genetic alterations as well as established cell lines such as MDA231. Cells expressing hTERT, SV40 T antigen, and Ras^{V12G} were derived from primary human mammary tissue samples.[1] These cells were transplanted together with SIPS or control fibroblasts as described for MDA231 cells (2 × 10^6 fibroblasts and 2 × 10^6 genetically modified mammary cells). At 10 days, xenografts formed with SIPSF were larger than xenografts formed with control fibroblasts or xenografts without fibroblasts (28 ± 4, 14 ± 3.1, and 8.7 ± 1.3 mm^3, respectively; P < 0.05 for SIPSF versus control fibroblasts and for SIPSF versus no fibroblasts). We conclude that the stimulatory effect of SIPSF on cancer cell growth *in vivo* is not confined to effects on established cancer cell lines like MDA231 and PC-3.

Fate of cotransplanted fibroblasts in xenografts. Because SIPSF cannot divide, we may assume that they exert their growth stimulatory effects at an early stage of xenograft growth before they become diluted by the proliferation of tumor cells. We did not know if control fibroblasts would similarly become diluted or if they may proliferate during growth of the xenograft. To investigate this, we cotransplanted MDA231 cells with control or SIPSF that

[1] S. Liang and P.J. Hornsby, unpublished observations.

express GFP as a marker (Fig. 3). We confirmed that GFP-expressing SIPSF increased the volume of xenografts sacrificed on day 14 (Fig. 3*A*). The xenografts were photographed at intervals using 470-nm illumination (Fig. 3*B*). The xenografts became progressively less fluorescent over time. This is consistent with dilution of GFP-expressing fibroblasts during xenograft growth. We confirmed this using immunostaining of sections from 14-day tumors (Fig. 3*C*). GFP-expressing cells were detected in MDA231/SIPSF and MDA231/CF xenografts, but GFP-positive cells were widely scattered in the tissues. Allowing for the greater size of MDA231/SIPSF xenografts, the total number of GFP-positive cells did not seem to be different between MDA231/SIPSF and MDA231/CF xenografts, indicating that little division of the control fibroblasts occurs. Neither SIPSF nor control fibroblasts form a substantial part of the cell population by day 14. Therefore, it is likely that any action of cotransplanted fibroblasts is exerted at the very early phase of xenograft growth.

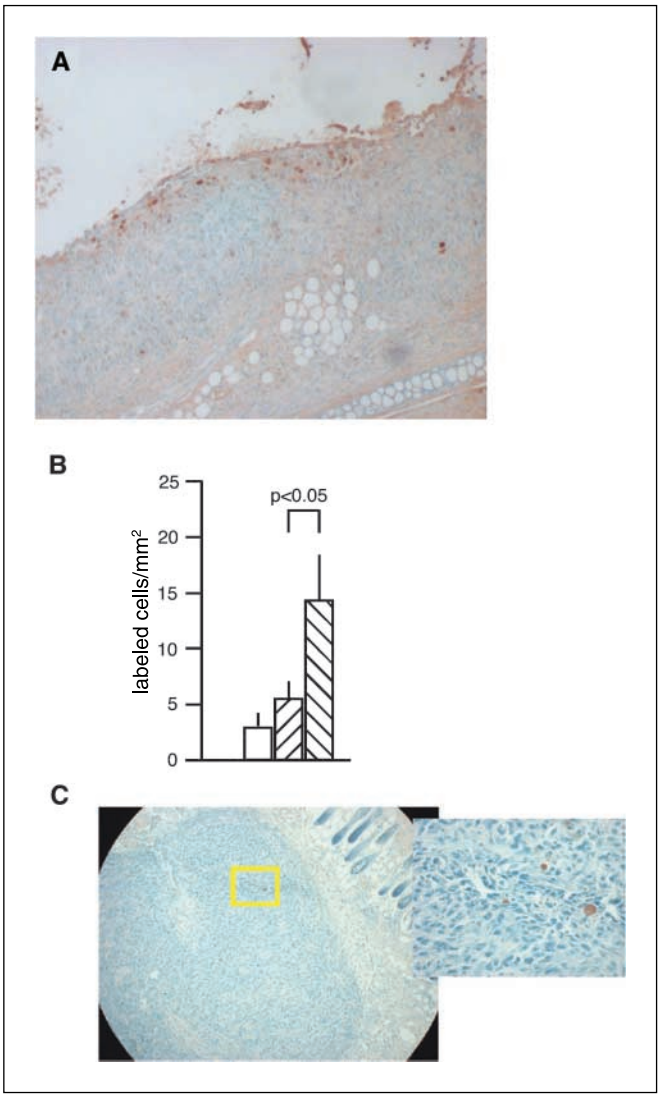

Figure 2. Stimulation of MDA231 xenograft growth by cotransplanted SIPSF is associated with stimulation of cell proliferation but not changes in apoptosis. *A,* proliferating cells (BrdUrd labeled) in a section of an MDA231/SIPSF xenograft, 5 d following cell transplantation. Magnification, ×170. *B,* proliferating cells in 5-day xenografts. *Open column,* MDA231 xenografts; *first hatched column,* MDA231/CF xenografts; *second hatched column,* MDA231/SIPSF xenografts. *C,* example of an MDA231/CF xenograft showing a small number of apoptotic cells visualized by *in situ* oligo ligation assay. *Yellow rectangle,* enlargement of area. Magnification, ×120; inset, ×550.

Role of MMPs in the stimulation of xenograft growth by SIPSF. The level of MMP-3 mRNA was ~24-fold greater in SIPS HCA2 fibroblasts than in control fibroblasts; MMP-1 mRNA was ~11-fold greater (Fig. 4*A*). SIPSF showed a slightly higher level of MMP-2 mRNA (Fig. 4*A*) but did not significantly overexpress MMP-9 and MMP-10 (data not shown). The serine proteases urokinase-type plasminogen activator (uPA) and tissue-type PA were elevated (~4-fold), and plasminogen activator inhibitor-1 was slightly increased. Levels of mRNAs for the inflammatory cytokines interleukin-1β (IL-1β), IL-1α, MCP-1 (Fig. 4*A*), and RANTES (data not shown) were elevated 10- to 20-fold. Transforming growth factor-β1 did not change significantly. HGF mRNA was elevated ~16-fold. Among matrix protein mRNAs, fibronectin was elevated ~2-fold (Fig. 4*A*), but elastin was unchanged (data not shown).

These senescent cell products are secreted factors. We used two types of antibody arrays to detect secreted products in conditioned medium. Using a human MMP antibody array, we confirmed that MMP-3 is produced in greater quantities by SIPSF, and that MMP-1 was also elevated (Fig. 4*B*). Data from the MMP antibody array also showed that tissue inhibitor of metalloproteinase-1 (TIMP-1) and TIMP-2 were produced in greater amounts by control fibroblasts. Data from a human cytokine antibody array showed that MCP-1 and RANTES were elevated in conditioned medium from SIPSF (Fig. 4*B*). Additionally, levels of HGF in conditioned medium were measured by ELISA (Fig. 4*C*). The level was much higher in medium from cultures of SIPSF.

Previous studies have often employed irradiated fibroblasts in cotransplantation xenograft studies, with variable results (22, 23, 29). We investigated whether irradiated HCA2 fibroblasts could act in MDA231 xenografts like SIPSF. Irradiated HCA2 fibroblasts showed a reduction in colony-forming ability of >100-fold. Irradiated cultures showed an increase in the number of SA-βgal$^+$ cells (from 0% in control cultures to ~10% of cells), which was nevertheless much less than the abundance in cultures of SIPSF, in which almost all cells were SA-βgal$^+$. When cotransplanted with MDA231 cells, irradiated fibroblasts did not significantly increase the size of xenografts at 9 days. We also measured mRNA levels for MMP-1, MMP-2, MMP-3, MMP-9, MMP-10, uPA, and HGF and found no significant increases in mRNA levels over control cells. We conclude that the growth stimulatory effect of SIPSF depends on factors other than simply entering a terminally nondividing state, which they share with irradiated fibroblasts. The inability of irradiated fibroblasts to stimulate xenograft growth suggests that changes in expression of genes such as *MMP* and *HGF* may be necessary for the growth stimulatory effect.

We also tested the potential for a growth-stimulatory effect of MDA231 cells, which had been treated with bleomycin, the agent used to induce SIPS in fibroblasts. A senescence-like state may be induced in MDA231 cells by DNA-damaging agents (42), although it should be noted that not all aspects of senescence are observed. Bleomycin-treated MDA231 cells and untreated MDA231 cells were mixed (2×10^6 treated and 2×10^6 untreated) and transplanted s.c. These xenografts did not exhibit an increased rate of growth in comparison with those formed from MDA231 cells alone. Levels of mRNAs for MMP-1, MMP-2, MMP-3, MMP-9, MMP-10, uPA, and HGF were not significantly affected by bleomycin treatment. Thus, both these data and the results with irradiated fibroblasts suggest that changes in expression of MMPs may be necessary for the growth-stimulatory effect in xenografts.

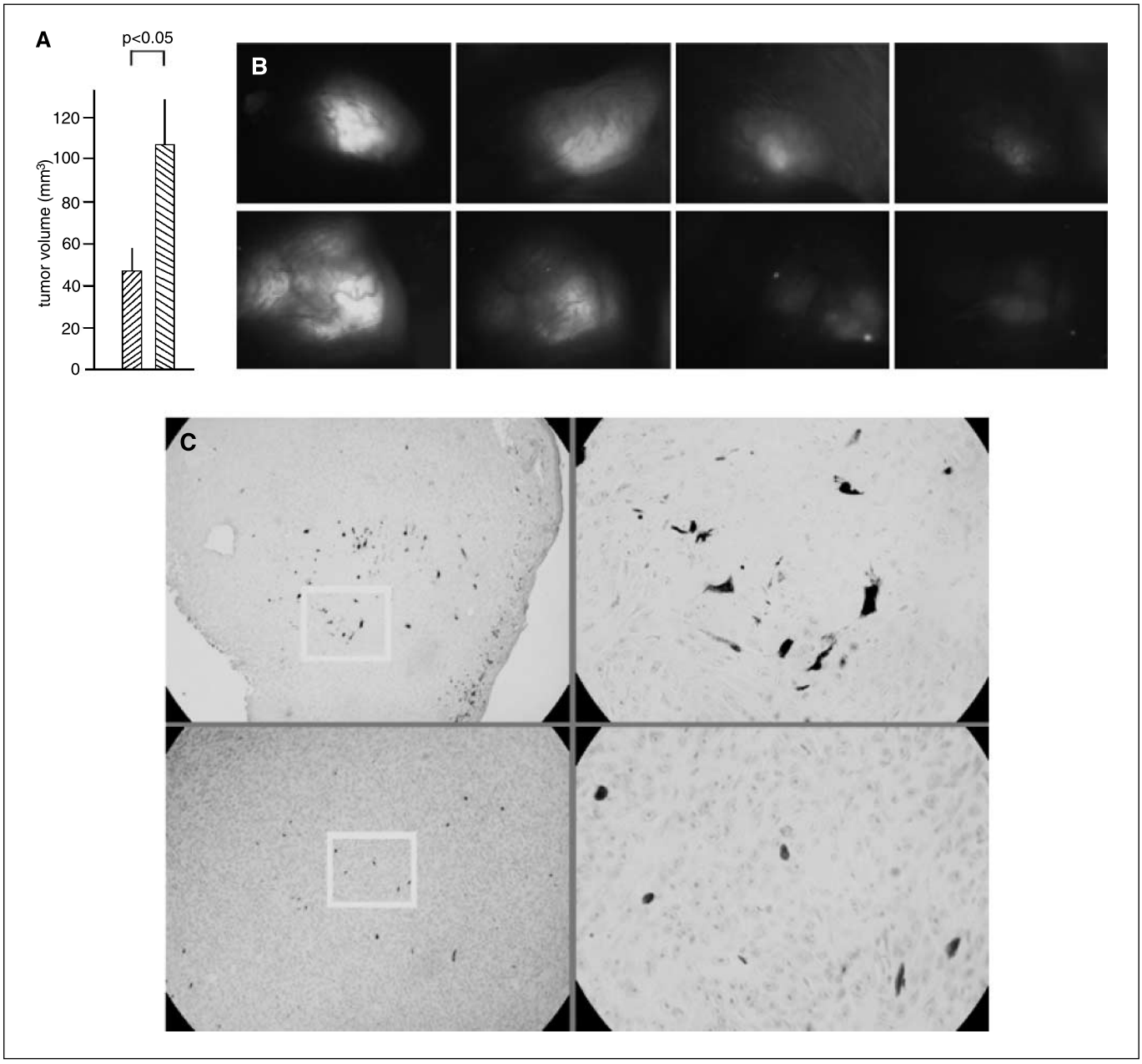

Figure 3. Fate of cotransplanted fibroblasts in MDA231 xenografts. MDA231 cells (10^6) were cotransplanted with 10^6 control HCA3-GFP fibroblasts (*CF*) or 10^6 SIPS HCA3-GFP fibroblasts (SIPSF). *A,* confirmation that MDA231/SIPSF xenografts are larger than MDA231/CF xenografts at 14 d when HCA3-GFP fibroblasts were used. Measurement made from histologic sections. *B,* change in fluorescence of xenografts over time. *Top,* an example of an MDA231/CF xenograft; *bottom,* an example of an MDA231/SIPSF xenograft. Fluorescence was photographed through the skin using a 470-nm wavelength illumination (*left* to *right,* 4, 7, 9, and 11 d). Magnification, ×10. *C,* sections of 14-d xenografts stained with an antibody against GFP. *Top,* MDA231/CF xenograft; *bottom,* MDA231/SIPSF xenograft. *Rectangle,* enlargement. Magnification, ×120; enlargement, ×450.

An MMP inhibitor impairs the effect of SIPSF on tumor growth *in vivo* but not *in vitro*. We used a broad-spectrum MMP inhibitor, GM6001 (43), to test the hypothesis that products of SIPSF that stimulate xenograft growth include MMPs. Zymography showed that conditioned medium from SIPSF has several proteins that are capable of digesting the in-gel substrate, casein (Fig. 5*A*). The inclusion of GM6001 in the reaction buffer inhibited the activity of one or more proteins in the 50- to 70-kDa size range. Although these bands have not been proven to be MMPs, this experiment shows that the majority of the proteolytic activity of SIPSF products is inhibitable by an agent that is active against MMPs.

We then investigated if GM6001 affected SIPSF-stimulated growth of MDA231 xenografts. The inhibitor was incorporated into transplants as described in Materials and Methods. Six groups of animals received various types of transplants; four groups were sacrificed at 5 days (MDA231/SIPSF ± GM6001 and MDA231/CF ± GM6001) and two groups at 9 days (MDA231/SIPSF ± GM6001). As anticipated, MDA231/SIPSF xenografts were significantly larger than MDA231/CF xenografts at 5 days (Fig. 4*B*). The difference was abolished by the inclusion of GM6001 in the transplant. The decreased size resulted from a decrease in the volume of the fluid portion of the xenografts (50.8% of the volume of MDA231/SIPSF

xenografts was occupied by fluid; GM6001 treatment reduced this to 28.3%, which is very similar to the value of 27.5% in MDA231/CF xenografts). Our observations above suggested that the growth stimulatory effect of SIPSF is evidenced by increased proliferation of tumor cells on day 5. Inclusion of GM6001 in the transplant greatly reduced the percentage of proliferating cells in the solid tissue portion of the xenograft (Fig. 5*C*). At 9 days, GM6001-treated MDA231/SIPSF xenografts were also smaller than untreated xenografts (Fig. 5*D*). Differences between treated and untreated xenografts diminished thereafter presumably because the growth of MDA231/SIPSF xenografts slows down as tumors reach larger sizes, as shown above (Fig. 1*A*).

If GM6001 reduces cell proliferation in xenografts by changing the ability of SIPSF products to digest extracellular matrix and cause fluid accumulation, it would not be anticipated that it would have an effect on SIPSF-stimulated cell proliferation in culture. We tested this in a model in which tumor or other cells are plated on top of a lawn of SIPS or control fibroblasts (30). The target cells were GFP or YFP expressing so that we could count the number of those cells independently of cells within the fibroblast lawn. SIPSF stimulated the proliferation of MDA231 cells as well as human hepatoma cells (Hep3B) and human prostate cancer cells (PC-3; Fig. 6*A*). Interestingly, SIPSF exerted a smaller effect on proliferation of a nontumorigenic cell line, hTERT-immortalized bovine adrenocortical cells (ref. 38; Fig. 6*A*). GM6001 did not inhibit the stimulation of cell proliferation observed for MDA231 cells in the presence of SIPSF (Fig. 6*B*). This indicates that the products of SIPSF that stimulate proliferation of target cells in culture are not likely to include MMPs. However, we showed that HGF, another SIPSF product (36), is likely to be one of the agents that acts to increase the growth of target cells in this cell culture model. When a neutralizing anti-HGF antibody was added to the cultures, the growth-stimulatory effect of SIPSF on MDA231 and PC-3 cells was partially inhibited (Fig. 6*C*). The inhibition could be reversed with recombinant HGF.

Discussion

Fibroblasts that have been forced into senescence by damage to their DNA, a form of SIPS, increased the growth of cancer cells in a cotransplantation xenograft model. SIPSF, like fibroblasts that become senescent by telomere shortening, show dramatic changes in gene expression, indicative of an inflammation/tissue injury response. Proteins that are increased as part of this response, including MMPs, are implicated in the action of senescent cells on xenograft growth. Our data support the hypothesis that the extent of stimulation of cancer cell growth by cotransplanted fibroblasts is proportional to the extent of changes in gene expression. A terminally nondividing state per se was insufficient. Fibroblasts rendered incapable of further cell division by high-dose γ radiation, as often used to prepare cells to use as feeder layers, did not support increased xenograft growth, but these cells were also not

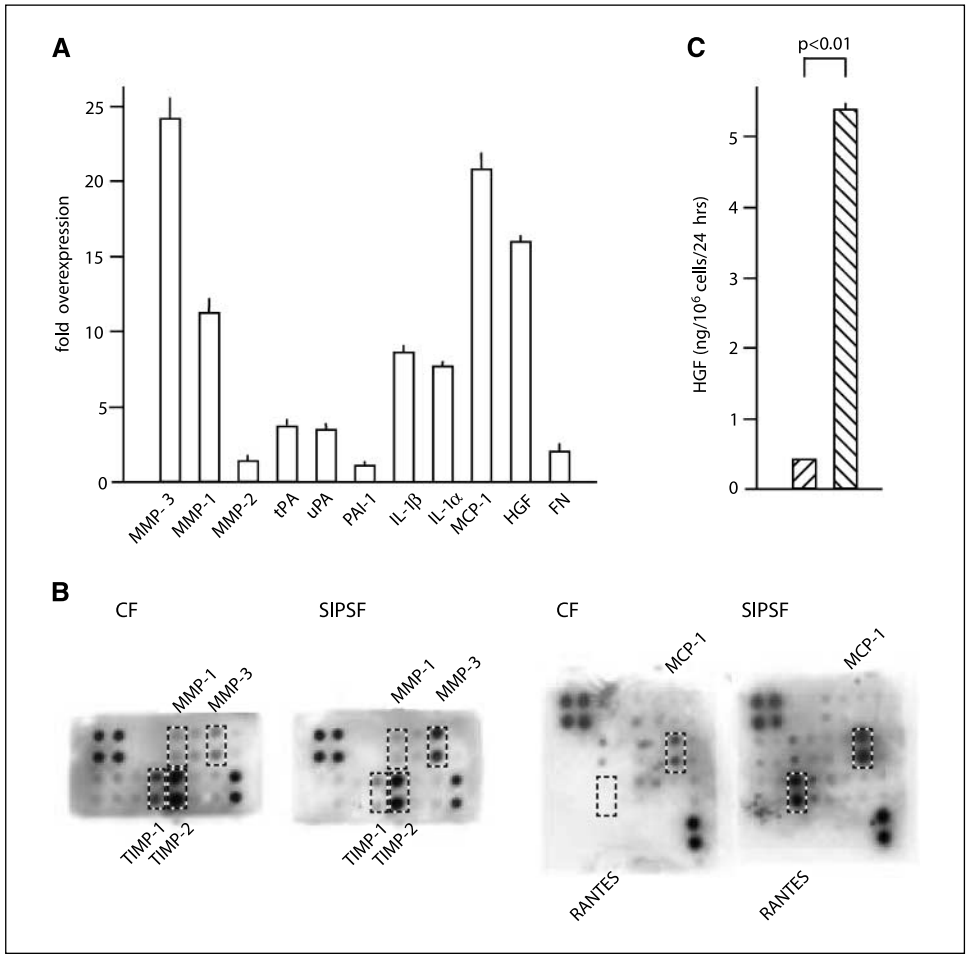

Figure 4. Changes in gene expression and protein secretion in SIPS versus control HCA2 fibroblasts. *A,* RNA was harvested from SIPS and control HCA2 fibroblasts and was assayed for levels of the indicated mRNAs by real-time PCR. Increase in the mRNA levels in the SIPSF RNA samples over the levels in control fibroblast samples ($n = 2–5$). *B,* differences in secreted proteins assayed by antibody arrays. Bleomycin-treated HCA2 fibroblasts (2.5×10^6; SIPSF) or control fibroblasts were incubated in 10 mL serum-free DMEM for 5 d. The conditioned medium was collected and was used in incubations with antibody arrays as described in Materials and Methods. Results for a human MMP array (*left*) and a human cytokine array (*right*). Positions of immobilized antibodies to MMP-1 and MMP-3, TIMP-1 and TIMP-2, RANTES, and MCP-1. Other spots are positive controls or MMPs/cytokines that were not detectable above background. *C,* differences in secreted levels of HGF assayed by ELISA. Bleomycin-treated HCA2 fibroblasts (5×10^5) or control fibroblasts were incubated in 0.5 mL serum-containing DMEM for 2 d. *Left column,* conditioned medium from untreated HCA2 fibroblasts; *right column,* conditioned medium from SIPS HCA2 fibroblasts.

made senescent by this treatment. These results do not preclude the likelihood that some irradiation protocols produce a larger proportion of senescent cells in the population, and that those cells may contribute to specific effects of irradiated versus nonirradiated cells in xenografts (29, 44).

The major novel finding in these experiments is that senescent cells cause early tissue injury when cotransplanted with cancer cells in a xenograft model. The damage is observed as fluid accumulation, a form of localized edema that is characteristic of inflammation/tissue injury (45). Although the structure of the xenograft is damaged by the presence of senescent cells, the cancer cells are stimulated to proliferate. Subsequently, xenografts formed by cotransplantation of senescent fibroblasts with cancer cells grow more rapidly than xenografts containing control fibroblasts or xenografts without fibroblasts. Although it is already established that the gene expression profile of senescent fibroblasts resembles that of fibroblasts in inflammation/tissue injury, these experiments show directly that senescent cells can damage the structure of surrounding tissues. Whereas normal tissue reacts to inflammation/injury with a series of changes that eliminate the damage and restore normal structure and function, cancer cells react with enhanced cell proliferation.

We do not yet know the extent to which cells that reach a senescent state *in situ* in tissues may exert a protumorigenic effect. However, there is epidemiologic evidence for an increased probability of cancers in diseases involving circulatory problems such as diabetic ulcers. Patients with chronic venous leg ulcers have a relative risk of 5.8 versus controls for a diagnosis of squamous cell carcinoma (SCC); the mean duration of the ulcers before the development of SCC was 25.4 years (46). SCCs occurred within or at the base of the ulcer. Senescent cells occur within ulcers (6), although it is unproven that they contribute to SCCs occurring within ulcers, investigating the possibility of a causal association will be an important topic for future studies.

In these experiments, the predominant alteration of tissue structure caused by senescent cells was the accumulation of extracellular fluid. Increased microvascular permeability, extravasation of plasma constituents and cells, and subsequent accumulation of extracellular fluid are commonly observed effects of localized tissue injury. Many of these effects are mediated by MMPs (11). MMPs directly injected into tissues also cause local damage and fluid accumulation (12).

The early increase in proliferating cells in the tissue adjacent to the central fluid in the xenografts suggests that it is the exposure to factors in extracellular fluid that enhances the subsequent growth of the cells. Both fluid accumulation and the subsequent senescent cell–mediated enhancement of xenograft growth were decreased by an MMP inhibitor. Do these results imply that increased fluid accumulation might mediate the effect of senescent fibroblasts on cancer development in tissues *in situ* rather than in a xenograft model? Whereas small numbers of senescent cells in tissues would not be expected to cause gross tissue damage, including significant extracellular fluid accumulation, it is plausible that they may be responsible for an MMP-driven increase in local microvascular permeability. Altered function of or damage to the microvasculature is a factor in many acute and chronic conditions (11). MMPs are implicated in many of these disorders; for example, in the central nervous system, MMPs are implicated in increased microvascular permeability and edema formation in several experimental models (47–49). Increased permeability (leakiness) is an established feature of capillaries in mature tumors, but its role in early tumor development is unknown (50, 51). Increased microvascular permeability may be involved in early effects of MMPs on incipient tumor cells because it exposes cells to serum components

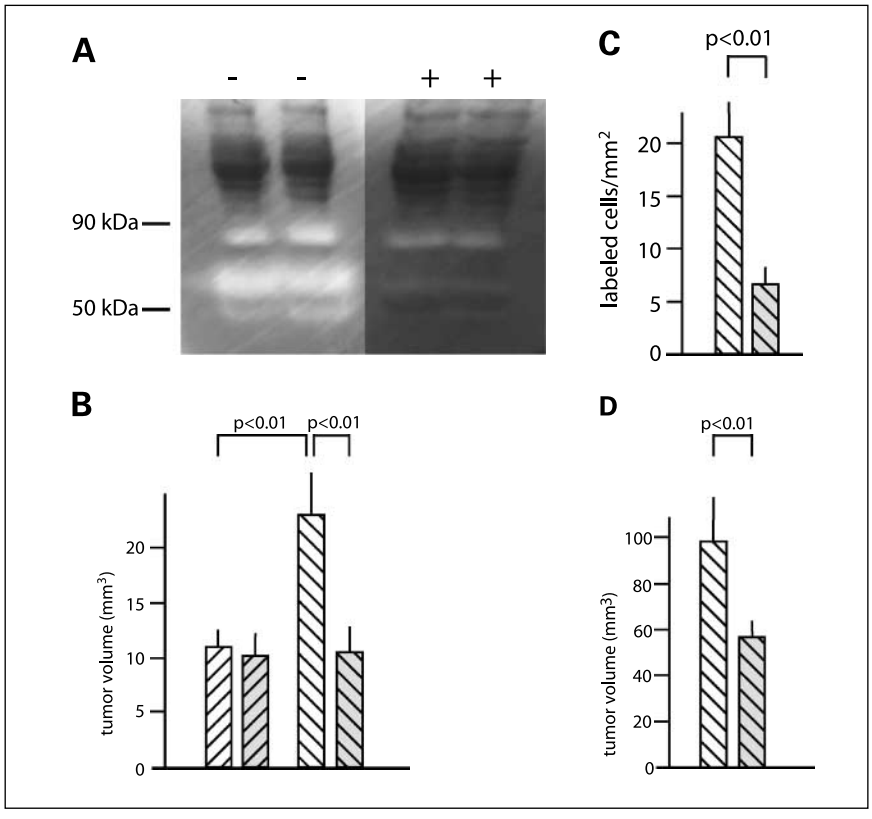

Figure 5. An MMP inhibitor abolishes the stimulation of MDA231 xenograft growth by SIPSF. *A,* zymograms of conditioned medium from SIPS HCA2 fibroblasts. Bleomycin-treated HCA2 fibroblasts (5×10^5) were cultured in 6-cm dishes and incubated with serum-free DMEM for 4 d. Proteins in medium samples were concentrated, as described in Materials and Methods, and were separated by electrophoresis on casein-containing gels. – and +, 1% DMSO (vehicle) or 25 μmol/L GM6001 was included in the reaction buffer before staining. *B,* MDA231/CF xenografts (*left two columns*) and MDA231/SIPSF xenografts (*right two columns*) from mice sacrificed at 5 d following cell transplantation (n = 6–8 each group). For xenografts in the groups represented by the gray-filled columns, the cotransplanted cells were mixed with 100 μmol/L GM6001 at the time of implantation beneath the skin of immunodeficient mice (see Materials and Methods for details). *C,* cell proliferation in 5-d xenografts assessed by Ki-67 labeling. MDA231/SIPSF xenografts with (*gray-filled column*) or without the inclusion of 100 μmol/L GM6001 in the transplants. *D,* MDA231/SIPSF xenografts from mice sacrificed at 9 d following cell transplantation with (*gray-filled column*) or without the inclusion of 100 μmol/L GM6001 in the transplants (n = 6–7 each group).

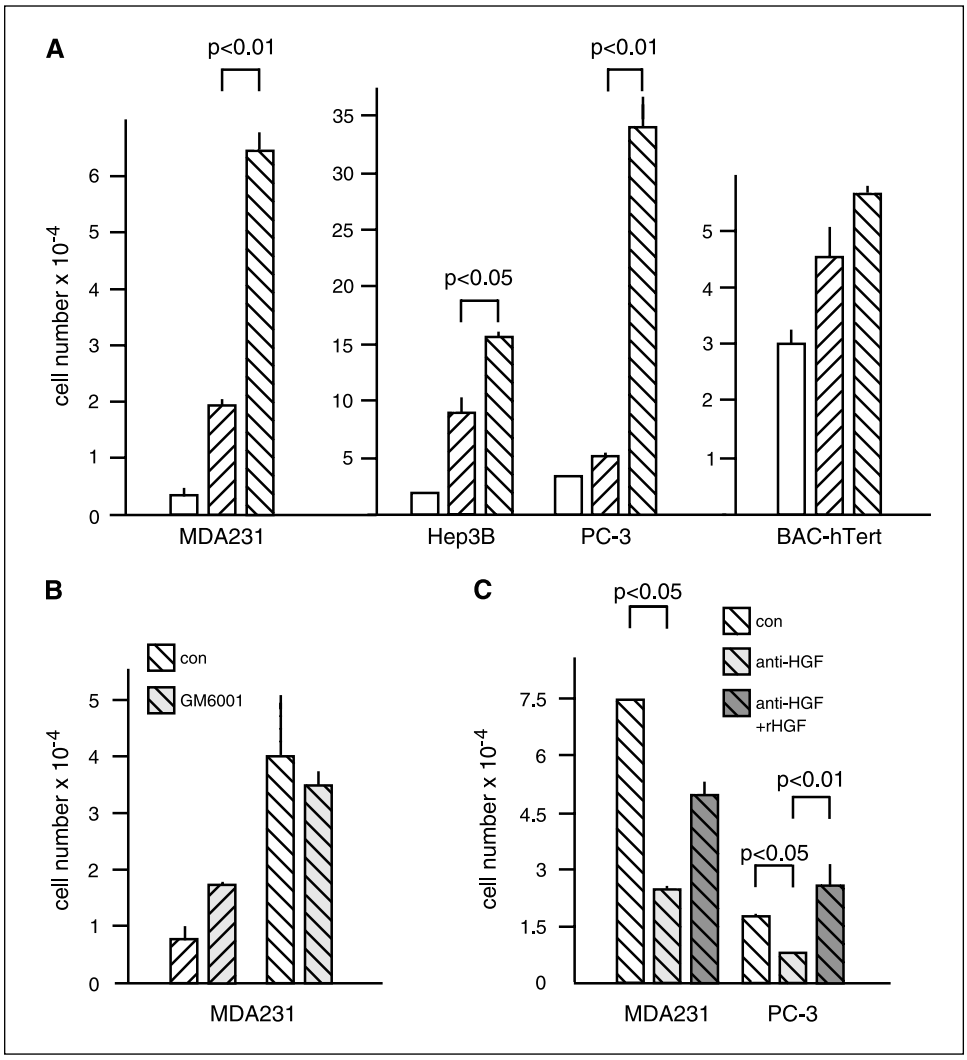

Figure 6. Stimulation of cell proliferation in culture by SIPSF does not result from production of MMPs but results in part from secretion of HGF. *A,* various cell lines were plated either on tissue culture plastic (*open column*) or on a confluent lawn of control HCA2 fibroblasts (*first hatched column*) or on a confluent lawn of SIPSF (*second hatched column*). Cells were allowed to proliferate for various periods of time and were then counted using GFP or YFP fluorescence. *Left* to *right,* MDA231 (12 d), Hep3B (8 d), PC-3 (8 d), and hTERT-immortalized bovine adrenocortical cells (BAC-hTert; 12 d). *B,* MDA231 cells plated on control (*first two columns*) or SIPSF (*second two columns*) with or without the addition of 25 μmol/L GM6001 to the medium and were allowed to proliferate for 8 d. *C,* MDA231 (5×10^3 cells) or PC-3 (5×10^3 cells) were plated on 10^5 SIPS HCA2 fibroblasts and allowed to proliferate for 9 d in the presence of 25 μg/mL control immunoglobulin, 25 μg/mL anti-HGF monoclonal antibody, or anti-HGF plus 200 ng/mL recombinant HGF.

from which they are normally shielded. For example, proteases, such as thrombin, are potent mitogens for many cell types, but exposure to thrombin is normally prevented by the barrier function of the capillary endothelium (52). Senescent cells in tissues might cause localized increases in the capillary permeability, thereby exposing adjacent cells to chronically elevated levels of serum components that increase cell proliferation.

Moreover, chronic microvascular injury could expose cells to blood components that cause DNA damage. Although the potential for such exposure to occur as a result of senescent cells in tissues is unknown, it has been shown that more acute, severe microvascular injury, such as that occurring in ischemia/reperfusion, causes DNA damage in cells of affected tissues (53). DNA damage could promote the full malignant conversion of preneoplastic cells. For example, SCp2 mouse mammary epithelial cells did not form tumors when transplanted alone in immunodeficient mice, but tumors arose with long latency in some animals when the cells were cotransplanted with senescent fibroblasts (30). This is consistent with a role for senescent cells in promoting preneoplastic SCp2 cells to full malignancy via DNA damage and consequent additional mutations. DNA damage caused by neighboring senescent cells might not only increase the risk that adjacent epithelial cells will undergo additional mutations but also may increase the potential for cancer initiation and promotion by causing more stromal cells to become senescent. It is also possible that senescent cells promote the growth of premalignant cells by providing a microenvironment that permits the growth of premalignant cells per se or of variants in the premalignant cell population. Supporting this concept, we found that SIPSF enhance the local growth of human cells with genetic modifications that do not lead to full malignancy.[2]

Our data also support a direct action of senescent cells on tumor cell proliferation via the secretion of mitogens such as HGF. As shown by others, we found that HGF was produced in greatly increased amounts by cells in stress-induced senescence (36). In contrast to MMPs, HGF directly increased tumor cell proliferation in monolayer culture. We did not find evidence that MMPs directly stimulate target cancer cell growth in coculture on conventional tissue culture plastic. However, stimulation of the growth of MDA-MB-231 cells by SIPSF in a three-dimensional coculture system was decreased by inhibition of MMP activity (21). These data suggest that senescent cells may exert effects via indirect actions, including tissue damage and matrix disruption, and also by direct actions,

[2] Unpublished observations.

including the secretion of mitogens (13, 20, 36, 54). Mitogenic senescent-cell products could act in synergy with agents such as MMPs that act indirectly via tissue damage. In summary, these experiments support the concept that the protumorigenic effect of senescent cells represents one form of the influence of inflammation and chronic injury on the development of cancer (32).

Acknowledgments

Received 9/17/2006; revised 1/2/2007; accepted 1/26/2007.

Grant support: National Institute on Aging grants AG12287 and AG20752 and Senior Scholar Award from the Ellison Medical Foundation. Support by the San Antonio Cancer Institute Cancer Center (P30 CA54174) is also acknowledged.

The costs of publication of this article were defrayed in part by the payment of page charges. This article must therefore be hereby marked *advertisement* in accordance with 18 U.S.C. Section 1734 solely to indicate this fact.

References

1. Shay JW, Wright WE. Senescence and immortalization: role of telomeres and telomerase. Carcinogenesis 2005; 26:867–74.
2. Campisi J. Senescent cells, tumor suppression, and organismal aging: good citizens, bad neighbors. Cell 2005;120:513–22.
3. Shay JW, Roninson IB. Hallmarks of senescence in carcinogenesis and cancer therapy. Oncogene 2004;23: 2919–33.
4. Kahlem P, Dorken B, Schmitt CA. Cellular senescence in cancer treatment: friend or foe? J Clin Invest 2004; 113:169–74.
5. Ben-Porath I, Weinberg RA. When cells get stressed: an integrative view of cellular senescence. J Clin Invest 2004;113:8–13.
6. Wlaschek M, Scharffetter-Kochanek K. Oxidative stress in chronic venous leg ulcers. Wound Repair Regen 2005;13:452–61.
7. Funk WD, Wang CK, Shelton DN, Harley CB, Pagon GD, Hoeffler WK. Telomerase expression restores dermal integrity to *in vitro*-aged fibroblasts in a reconstituted skin model. Exp Cell Res 2000;258:270–8.
8. West MD, Pereira-Smith OM, Smith JR. Replicative senescence of human skin fibroblasts correlates with a loss of regulation and overexpression of collagenase activity. Exp Cell Res 1989;184:138–47.
9. Millis AJ, Hoyle M, McCue HM, Martini H. Differential expression of metalloproteinase and tissue inhibitor of metalloproteinase genes in aged human fibroblasts. Exp Cell Res 1992;201:373–9.
10. Shelton DN, Chang E, Whittier PS, Choi D, Funk WD. Microarray analysis of replicative senescence. Curr Biol 1999;9:939–45.
11. Alexander JS, Elrod JW. Extracellular matrix, junctional integrity and matrix metalloproteinase interactions in endothelial permeability regulation. J Anat 2002; 200:561–74.
12. Newman TA, Woolley ST, Hughes PM, Sibson NR, Anthony DC, Perry VH. T-cell- and macrophage-mediated axon damage in the absence of a CNS-specific immune response: involvement of metalloproteinases. Brain 2001;124:2203–14.
13. Elenbaas B, Weinberg RA. Heterotypic signaling between epithelial tumor cells and fibroblasts in carcinoma formation. Exp Cell Res 2001;264:169–84.
14. Tlsty TD, Hein PW. Know thy neighbor: stromal cells can contribute oncogenic signals. Curr Opin Genet Dev 2001;11:54–9.
15. Lynch CC, Matrisian LM. Matrix metalloproteinases in tumor-host cell communication. Differentiation 2002; 70:561–73.
16. van Kempen LC, Ruiter DJ, van Muijen GN, Coussens LM. The tumor microenvironment: a critical determinant of neoplastic evolution. Eur J Cell Biol 2003;82:539–48.
17. Bhowmick NA, Neilson EG, Moses HL. Stromal fibroblasts in cancer initiation and progression. Nature 2004;432:332–7.
18. Tang Y, Nakada MT, Kesavan P, et al. Extracellular matrix metalloproteinase inducer stimulates tumor angiogenesis by elevating vascular endothelial cell growth factor and matrix metalloproteinases. Cancer Res 2005;65:3193–9.
19. Giambernardi TA, Grant GM, Taylor GP, et al. Overview of matrix metalloproteinase expression in cultured human cells. Matrix Biol 1998;16:483–96.
20. Parrinello S, Coppe JP, Krtolica A, Campisi J. Stromal-epithelial interactions in aging and cancer: senescent fibroblasts alter epithelial cell differentiation. J Cell Sci 2005;118:485–96.
21. Tsai KK, Chuang EY, Little JB, Yuan ZM. Cellular mechanisms for low-dose ionizing radiation-induced perturbation of the breast tissue microenvironment. Cancer Res 2005;65:6734–44.
22. Picard O, Rolland Y, Poupon MF. Fibroblast-dependent tumorigenicity of cells in nude mice: implication for implantation of metastases. Cancer Res 1986;46: 3290–4.
23. Camps JL, Chang S-M, Hsu TC, et al. Fibroblast-mediated acceleration of human epithelial tumor growth *in vivo*. Proc Natl Acad Sci U S A 1990;87:75–9.
24. Noel A, De Pauw-Gillet MC, Purnell G, Nusgens B, Lapiere CM, Foidart JM. Enhancement of tumorigenicity of human breast adenocarcinoma cells in nude mice by Matrigel and fibroblasts. Br J Cancer 1993;68:909–15.
25. Brouty-Boye D, Raux H. Differential influence of stromal fibroblasts from different breast tissues on human breast tumour cell growth in nude mice. Anticancer Res 1993;13:1087–90.
26. Thomas M, Northrup SR, Hornsby PJ. Adrenocortical tissue formed by transplantation of normal clones of bovine adrenocortical cells in *scid* mice replaces the essential functions of the animals' adrenal glands. Nat Med 1997;3:978–83.
27. Olumi AF, Grossfeld GD, Hayward SW, Carroll PR, Tlsty TD, Cunha GR. Carcinoma-associated fibroblasts direct tumor progression of initiated human prostatic epithelium. Cancer Res 1999;59:5002–11.
28. Thomas M, Hornsby PJ. Transplantation of primary bovine adrenocortical cells into scid mice. Mol Cell Endocrinol 1999;153:125–36.
29. Kuperwasser C, Chavarria T, Wu M, et al. Reconstruction of functionally normal and malignant human breast tissues in mice. Proc Natl Acad Sci U S A 2004; 101:4966–71.
30. Krtolica A, Parrinello S, Lockett S, Desprez PY, Campisi J. Senescent fibroblasts promote epithelial cell growth and tumorigenesis: a link between cancer and aging. Proc Natl Acad Sci U S A 2001;98:12072–7.
31. Noel A, Hajitou A, L'Hoir C, et al. Inhibition of stromal matrix metalloproteases: effects on breast-tumor promotion by fibroblasts. Int J Cancer 1998;76: 267–73.
32. Coussens LM, Werb Z. Inflammation and cancer. Nature 2002;420:860–7.
33. Robles SJ, Adami GR. Agents that cause DNA double strand breaks lead to p16(INK4A) enrichment and the premature senescence of normal fibroblasts. Oncogene 1998;16:1113–23.
34. Toussaint O, Remacle J, Dierick JF, et al. From the Hayflick mosaic to the mosaics of ageing. Role of stress-induced premature senescence in human ageing. Int J Biochem Cell Biol 2002;34:1415–29.
35. Parrinello S, Samper E, Krtolica A, Goldstein J, Melov S, Campisi J. Oxygen sensitivity severely limits the replicative lifespan of murine fibroblasts. Nat Cell Biol 2003;5:741–7.
36. Bavik C, Coleman I, Dean JP, Knudsen B, Plymate S, Nelson PS. The gene expression program of prostate fibroblast senescence modulates neoplastic epithelial cell proliferation through paracrine mechanisms. Cancer Res 2006;66:794–802.
37. Kumazaki T, Robetorye RS, Robetorye SC, Smith JR. Fibronectin expression increases during *in vitro* cellular senescence: correlation with increased cell area. Exp Cell Res 1991;195:13–9.
38. Sun B, Huang Q, Liu S, et al. Progressive loss of malignant behavior in telomerase-negative tumorigenic adrenocortical cells and restoration of tumorigenicity by human telomerase reverse transcriptase. Cancer Res 2004;64:6144–51.
39. Dimri GP, Lee XH, Basile G, et al. A biomarker that identifies senescent human cells in culture and in aging skin *in vivo*. Proc Natl Acad Sci U S A 1995;92:9363–7.
40. Popnikolov NK, Hornsby PJ. Subcutaneous transplantation of bovine and human adrenocortical cells in collagen gel in scid mice. Cell Transplant 1999;8:617–25.
41. Hornsby PJ, Yang L, Thomas M. Adrenocortical cell proliferation in a cell transplantation model: the role of SV40 T antigen. Endocr Res 2002;28:777–83.
42. Chang BD, Broude EV, Dokmanovic M, et al. A senescence-like phenotype distinguishes tumor cells that undergo terminal proliferation arrest after exposure to anticancer agents. Cancer Res 1999;59:3761–7.
43. Grobelny D, Poncz L, Galardy RE. Inhibition of human skin fibroblast collagenase, thermolysin, and *Pseudomonas aeruginosa* elastase by peptide hydroxamic acids. Biochemistry 1992;31:7152–4.
44. Ohuchida K, Mizumoto K, Murakami M, et al. Radiation to stromal fibroblasts increases invasiveness of pancreatic cancer cells through tumor-stromal interactions. Cancer Res 2004;64:3215–22.
45. Plante GE, Chakir M, Ettaouil K, Lehoux S, Sirois P. Consequences of alteration in capillary permeability. Can J Physiol Pharmacol 1996;74:824–33.
46. Baldursson B, Sigurgeirsson B, Lindelof B. Venous leg ulcers and squamous cell carcinoma: a large-scale epidemiological study. Br J Dermatol 1995;133:571–4.
47. Wang J, Tsirka SE. Neuroprotection by inhibition of matrix metalloproteinases in a mouse model of intracerebral haemorrhage. Brain 2005;128:1622–33.
48. Garg R, Chaudhuri A, Munschauer F, Dandona P. Hyperglycemia, insulin, and acute ischemic stroke: a mechanistic justification for a trial of insulin infusion therapy. Stroke 2006;37:267–73.
49. Lominadze D, Roberts AM, Tyagi N, Moshal KS, Tyagi SC. Homocysteine causes cerebrovascular leakage in mice. Am J Physiol 2006;290:H1206–13.
50. Baish JW, Netti PA, Jain RK. Transmural coupling of fluid flow in microcirculatory network and interstitium in tumors. Microvasc Res 1997;53:128–41.
51. Heldin CH, Rubin K, Pietras K, Ostman A. High interstitial fluid pressure-an obstacle in cancer therapy. Nat Rev Cancer 2004;4:806–13.
52. Macfarlane SR, Seatter MJ, Kanke T, Hunter GD, Plevin R. Proteinase-activated receptors. Pharmacol Rev 2001;53:245–82.
53. Hornsby PJ. Dysfunction of the adrenal cortex: an exploration of molecular mechanisms. J Organ Dysfunction 2005;1:69–77.
54. Martin TA, Parr C, Davies G, et al. Growth and angiogenesis of human breast cancer in a nude mouse tumour model is reduced by NK4, a HGF/SF antagonist. Carcinogenesis 2003;24:1317–23.